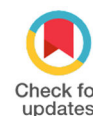


The Oriented Attachment Crystal Growth Model in Hydrothermal Synthesis of Magnetite (Fe_3O_4) nanoparticles



Ahmad Fadli^{1,*}, Amun Amri¹, Esty Octiana Sari¹, Sukoco¹, and Deden Saprudin²

¹Department of Chemical Engineering, Universitas Riau

²Department of Chemistry, Bogor Agricultural University

ABSTRACT: The magnetite nanoparticles (Fe_3O_4) are very promising nanomaterial to be applied as drug delivery due to their excellent superparamagnetic, biocompatibility and easily modified surface properties. Those properties are influenced by the structure and size of the material which depend on the synthesis condition. Studying the evolution of crystal growth can help understand the mechanisms and factors that play a role in it more systematically. The purpose of this research is to study the evolution of crystal growth of magnetite nanoparticles in the hydrothermal system and determine the crystal growth kinetics using the Oriented Attachment Growth model. Magnetite nanoparticles were synthesized using a hydrothermal method from FeCl_3 , citrate, urea and polyethylene glycol at 210°C for 1 - 12 hours at a various concentration of FeCl_3 (0.05 M, 0.10 M, and 0.15 M). The characterizations were conducted by X-ray Diffraction (XRD), Transmission Electron Microscope (TEM), Particle size analyzer (PSA), and Vibrating Sample Magnetometer (VSM). The XRD diffractogram indicated that the magnetite was begun to form at 3.5 hours synthesis. The crystallinity and the crystal size of magnetite rose with reaction time. The diameter of magnetite crystals was in the range of 9.4-30 nm. Characterization by TEM showed that the particles were formed from smaller particles which were then agglomerated. The characterization by PSA showed that an increase in FeCl_3 concentration made the particle size larger but the particle distribution narrower. PSA results also prove that the longer the reaction time, the more particle diameter increases will be. VSM result showed that the magnetite nanoparticle has superparamagnetic properties. The magnetite crystal growth can be fitted by the Oriented Attachment Growth model with an error of 29%.

Key words: Crystal growth, Drug delivery, Hydrothermal, Magnetite nanoparticles, Oriented attachment model

1. INTRODUCTION

Cancer is a major public health problem and the second leading cause of death globally. The latest update from the IARC (International Agency for Research on Cancer), the cancer burden rises to 18.1 million new cases and responsible for an estimated 9.6 million deaths in 2018 [1]. However, conventional treatments such as surgery, radiation, chemotherapy, and biologic therapies (immunotherapy) are limited by the accessibility to the tumor, the risk of operating on a vital organ, the spread of cancer cells throughout the body, and the lack of selectivity toward the tumor cells [2].

In recent times, the drug delivery has been developed as a new method for cancer therapy. The principle of this method is delivering the drug into the target site using a nanoparticle as a "vehicle". The advantages of nano drug delivery compared to conventional medication methods are (1) it has the ability to treat the specific targets in the body, (2) the dose of the drug is reduced, (3) the concentration of the drug at the nontarget sites is reduced, and (4) the side effects caused by drug toxicity in cells/nontarget tissues are reduced [2].

Magnetite nanoparticle (Fe_3O_4) is one of the materials that is a very promising candidate for being applied to drug delivery system due to its superparamagnetic and high-biocompatibility properties [3]. The controlled size and the morphology of nanoparticles are needed in drug delivery

system because it affects the accessibility, the time residence in the bloodstream and the toxicity in the human body [4, 5]. The synthesis of magnetite nanoparticles with controllable size and morphology are remain a challenge. The study of the evolution of crystal growth can help to understand the factors that influence the growth of crystals. An understanding of the factors that affect the crystal growth kinetics and microstructure development in nanocrystals is fundamental to control the nanoparticle properties [6]. It is important for the tailoring process of the nanoparticles to have uniform size and morphology [6].

[7] had been studied the effect of temperature on the evolution of crystal growth in the hydrothermal system and modeled it using Ostwald Ripening model. It is found that the crystal growth reaction was controlled by dissolution kinetics at the particle-matrix interface. However, it is known that in the nanoscale systems, the surface contributions to the total energy become increasingly important as the particle size decreases. Nanocrystals have a higher surface energy, which facilitates the "reaction" on the surface, such as the direct bonding and the crystallization among the particles namely oriented attachment (OA) pathway [8].

Received : April 30, 2019

Revised : June 22, 2019

Accepted : July 17, 2019

Here, we investigated the magnetite coarsening in the hydrothermal system using the oriented attachment approach.

2. EXPERIMENTAL

This study consisted of three main stages: (1) magnetite nanoparticles preparation using the hydrothermal method, (2) characterizations using XRD (X-ray diffraction), TEM (transmission electron microscope), PSA (particle size analyzer), and VSM (vibrating sample magnetometer) and (3) modeling the kinetics of magnetite crystal growth.

2.1 Synthesis of magnetite nanoparticles

The magnetite nanoparticles were synthesized using the hydrothermal method. The various concentrations of FeCl_3 (0.05 M, 0.10 M, and 0.15 M), 4 mmol of sodium citrate (0.10 M), and 6 mmol of urea (0.15M) were dissolved into the 40 cm³ of distilled water, then 0.1 g of PEG was added until it was completely dissolved. The solution was finally transferred into a Teflon-lined autoclave. The Teflon-lined autoclave was put into an oven and the temperature was set to 210°C. The reaction times used in this study were 1, 2, 3, 3.5, 5, 7, 9, and 12 hours. The black precipitate formed was separated by a bar magnet, then washed with water and ethanol, and dried at 60°C overnight. The black precipitates were characterized by XRD, TEM, PSA, BET analyzer and VSM.

2.2 Characterization

2.2.1 XRD characterization

Identification, crystallinity and size of nanoparticles were determined by XRD. Approximately 200 mg of sample was printed directly on aluminum measuring 2 × 2.5 cm². Samples were characterized using XRD instrument with Cu radiation light ($\lambda = 1.54 \text{ \AA}$) with a voltage of 40 kV and a current of 30 Ma at 2θ of 10–99.97°.

2.2.2 TEM characterization

The particles size, morphology, and aggregate were analyzed by transmission electron microscope (TEM JEOL JEM 1400) operated at 5 kV under vacuum.

2.2.3 Particle Size Analyzer (PSA) Characterization

The particle size distribution was analyzed by PSA (Beckman Coulter) at 25°C and the viscosity of 0.8878 cp in water for 30 minutes.

2.2.4 VSM characterization

Characteristics of magnetic nanoparticles were analyzed by Vibrating Sample Magnetometer (VSM) type VSM1.2H Oxford. Magnetization curves measured at room temperature with a magnetic field that varies in the range -1 to 1 Tesla.

2.3 Kinetic modeling of crystal growth

The Oriented Attachment (OA) crystal growth model explained the crystal growth based on the joining of crystal particles. The primary particles met with other primary particles forming secondary particles. The secondary particles met with the primary particles forming the tertiary particles and so on to form larger ones without the dissolution of either particle. The driving force of this process was attributed to the decrease in surface and grain boundary free energies [9]. The general equation of

Oriented Attachment crystal growth model was presented in equation 1:

$$D = \frac{D_0(\sqrt[3]{2k.t+1})}{(k.t+1)} \quad (1)$$

D was crystal diameter, D_0 was the diameter of crystal formed initially, K was constant and t was the time reaction. The K value was obtained from the intercept of the experimental data following equation:

$$\ln \left[(1-\alpha) \left[\frac{D_0}{D} \right]^3 \right] = \ln k + \ln t \quad (2)$$

Furthermore, the value of D and D_0 were obtained to the model curve. The experimental curve then matched with the model.

3. RESULTS AND DISCUSSION

3.1 Magnetic properties and VSM results

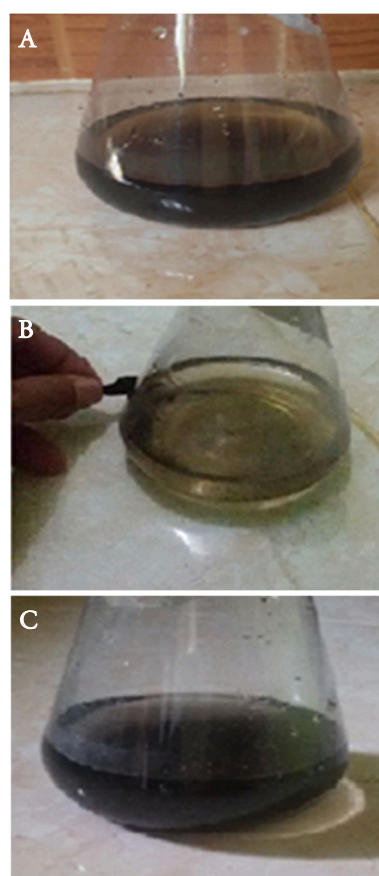


Fig. 1. The as-synthesized black precipitate disperse well in water (a) the precipitate interacts with external magnetic field (b) re-dispersible powder in the water after the magnetic field is removed (c)

The formation of magnetite nanoparticle is shown by the formation of black precipitate at 3.5 h synthesis (Fig. 1). The precipitate is well dispersed in water (Fig. 1a). These properties are expected in the development of drug delivery. The presence of PEG that has an -OH group on the surface makes the nanoparticles are hydrophilic and negatively charged. Thus, it makes the nanoparticles have a longer residence time in the bloodstream (high bioavailability)

because it corresponds to the nature of the plasma proteins which is also hydrophilic and negatively charged. In general, phagocytosis will occur in particles of non-polar (hydrophobic) and positively charged as it is considered as a foreign substance to the body. In addition, the presence of PEG on the surface of magnetite nanoparticles also prevents oxidation by the air and becomes a place for drug attachment [10, 11].

When it is brought closer to the external magnetic field, the precipitate interacts with magnetic field (Fig.1b). Magnetic properties of the precipitate appear when it is exposed to the external magnetic field and then disappear when the magnetic field is eliminated (Fig 1c). This shows that the magnetite has superparamagnetic properties.

The VSM hysteresis curve of the precipitated magnetic is depicted in Fig.2. There is a very narrow hysteresis loop with coercivity's (H_c) value of near zero (0.02T). This reaffirms that as-synthesized magnetite nanoparticle has superparamagnetic properties. This superparamagnetic properties gives advantages in drug delivery application such as easy to guide to the parts of body by external magnetic field and preventing the effects of agglomeration after the application of external magnetic fields [12].

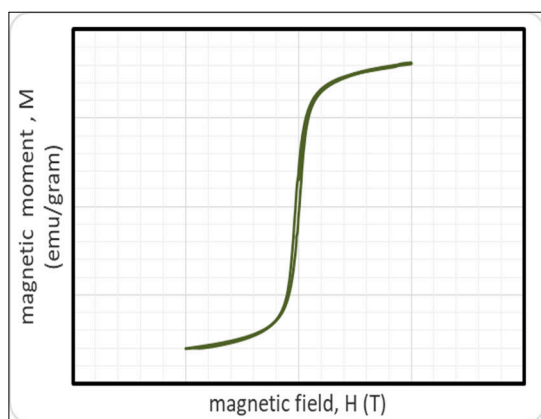


Fig. 2. Hysteresis curve of the as-synthesized magnetite nanoparticles

3.2 XRD analysis

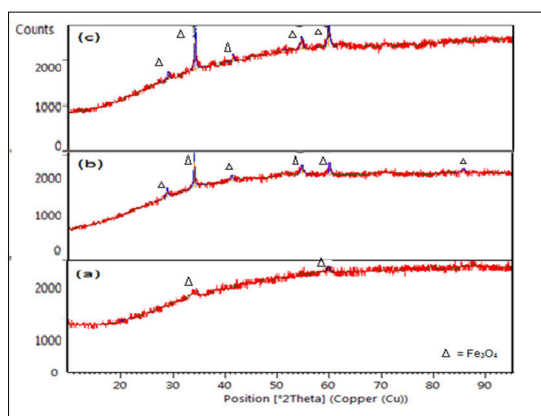


Fig. 3. The XRD pattern of as-synthesized magnetite at 210°C for 3.5 h (a), 5 h (b), and 12 h (c)

The XRD patterns match with the standard pattern of Fe_3O_4 with the highest intensities at 2θ 35.54°; 57.06°; and 62.66° which confirm that the precipitate is pure magnetite

(Fig.3). The intensity of the peak rises as the time increase, indicates an increasing in crystallinity of magnetite (Fig.3).

The XRD pattern of samples synthesized from various FeCl_3 concentrations are shown in Fig.4. All of sample patterns are well-matched with the standard pattern of Fe_3O_4 , indicate a pure Fe_3O_4 are formed in different concentration. The intensities of XRD peaks show higher intensity in higher concentrations, indicates higher crystallinity product was obtained from the higher concentration of FeCl_3 . However, the peak boardening decrease with higher concentration shows bigger crystallite size obtained in higher concentration of FeCl_3 .

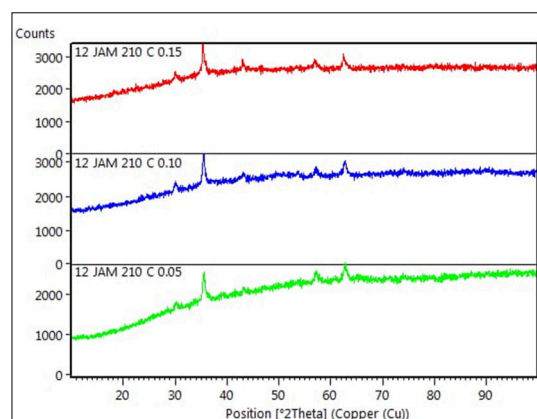


Fig. 4. Diffraction pattern of the as-synthesized samples at temperatures of 210 ° C 12 hours, FeCl_3 concentrations of (a) 0.05 M, (b) 0.10 M and (c) 0.15 M

3.3 TEM images analysis

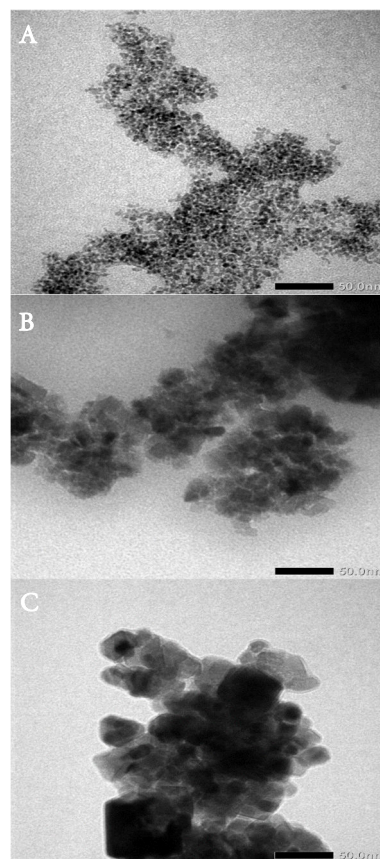


Fig. 5. TEM image of nanoparticles synthesized at temperature of 210 ° C at 3.5 h (a), 7 h (b), and 12 h (c) with magnification of 80,000X

The morphology of magnetite nanoparticles is shown by the TEM images (Fig. 5). TEM image shows that at 3.5 hours, thenano-sized particles formed are uniform in diameter, they are about less than 10 nm (Fig. 5a). It can be seen that at the initial formation step, the single crystal is formed. The dark region shows a high cristallinity and the light region shows a low cristallinity. The light region of particle is larger than the dark region indicatinga low cristallinity (high amorphouse phase) of nanoparticles formed at the initial formation as indicated in XRD data.

The 7 hours synthesis results particles which have less regulated morphology and agglomerated with the final diameter of about 100 nm (Fig. 5b). At 12 hours, the particles are more crystalline and the agglomeration still occur with the final diameter of more than 100 nm (Fig. 5c). The TEM image reveals that at longer reaction time, the initial particle coalesces to decrease the interfacial energy, as the basis of modeling with the Oriented Attachment approach. The agglomeration is not expected for drug delivery application due to anisotropy in pharmacology effect. However, magnetite nanoparticles obtained in this experimentare in accordance with the criteria of drug delivery, which are 10 nm - 200 nm [2].

3.4 PSA results

The Particle Size Analyzer (PSA) results are depicted in Fig 9 and Table 2. Based on Fig. 9, it can be seen that the different synthesis conditions produce different distribution of magnetite nanoparticles size. The particle size distributionof sample synthesized at 0.1 M reactant concentration is narrow (Fig 6a and 6c), while for sample synthesized at 0.15 M concentration the particle size distribution is wide indicating higher polydispersity (Fig. 6b).

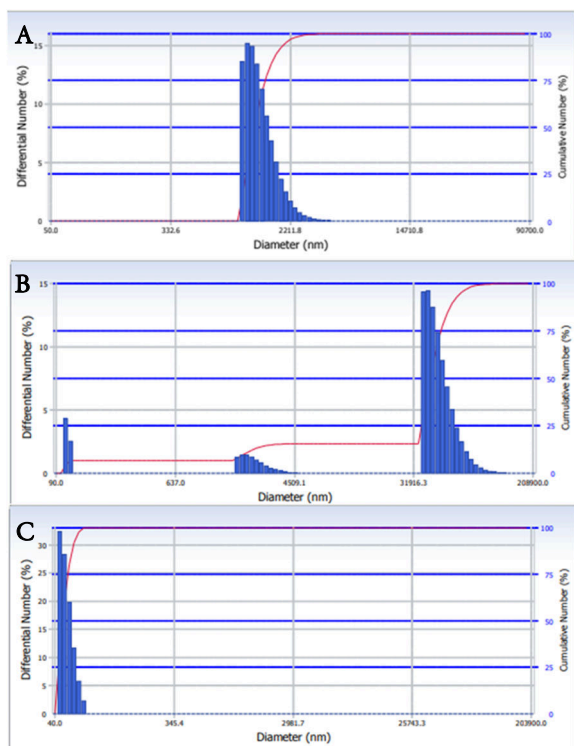


Fig. 6. Distribution of particle diameter of the as-synthesized magnetite at 210 ° C (a) 3.5 hours 0.10 M (b) 12 hours 0.10 M and (c) 12 hours 0.15M

Table 2 Particle size of the as-synthesized magnetite based on PSA characterization

Sum of particle size distribution at synthesis condition :					
0,1 M 3,5 h		0,1 M 12 h		0,15 M 12 h	
size (nm)	percentage (%)	size (nm)	percentage (%)	size (nm)	percentage (%)
<10	0	<10	0	<10	0
10	13	10 - 20	8.68	10 sd 20	0
11	15	20 - 30	5.41	20 sd 30	0
12	14	30 sd 40	41.69	30 sd 40	0
13	13.79	40 sd 50	25.12	40 sd 50	60.59
14	15.31	50 sd 60	7.5	50 sd 60	31.39
15 sd 20	26	60 sd 70	11.6	60 sd 70	8.02
> 20	2.9	> 70	4.4	> 70	0
total	100	total	100	total	100

Table 2 shows, for sample synthesized using 0.1 M reactant for 3.5 hours, the particle size in range of 10-20 nm is about 97%, while forthe sample synthesized for 12 hours s the particle size in range of 30-50 nm is about 66.81%.It also shows that the percentage of the small particle decreases by the time but the percentage of the bigger particles increases. It reveals a coarsening in the hydrothermal system as the longer reaction time with hypothetically Oriented Attachment path way. For the sample synthesized at reactant concentration of 0.15 M and 12 hours synthesis, the particle size in range of 40-70 nm is about 100%. Thus, it can be concluded that the higher concentration of FeCl_3 will produce larger particle diameter but narrower particle size distribution. PSA results also prove that the longer the reaction time, the more particle diameter increases will be. This also prove the occurrence of coalescence of small particles into large particles, seen from the reduced percentage of small particles formed after 12 hours compared to the percentage of small particles formed at 3.5 hours.

3.5 Modeling of magnetite nanoparticle crystals growth by Oriented Attachment (OA) approach

The XRD, TEM and PSA data show the tendency of the nanoparticle growth from combining small particles into larger particles through the agglomeration. To prove the occurrence of Oriented Attachment pathway in the process of magnetite crystal growth in hydrothermal system, modeling is made. Based on experimental data obtained from X-ray diffraction, the crystal diameters are determined by Scherres formula. Then, the k values are obtained from the concentrations of 0.05 M, 0.1 M and 0.15 M. From this k value the diameter of the model is determined by substituting the parameters D_0 and t (Equation 1). The plot of crystal diameter vs time at various reactant concentrations are shown in Fig 7.

In fig. 7, it can be seen that the crystal diameter from the experimental results on the increase in reaction time become closer to the model point. The elevation points issrink from the reaction time of 5, 7, 9 and 12 hours. It can be concluded that increasing reaction time the growth of magnetite crystals following the Oriented Attachment (OA) model. In different concentration treatments, the growth response of magnetite crystals is also different. At 0.15 M reactant for 5-hour synthesis, the percent of error reaches 29%. Whereas for 0.10 M and 0.05 M reactants, the error is of 19.15% and 9.6%, respectively. It can be seen that the experiment is

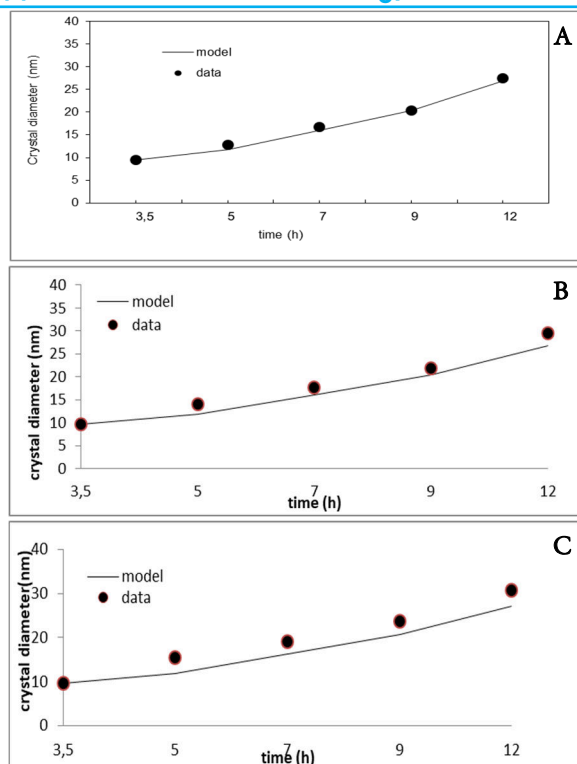


Fig. 7. Diameter of magnetite crystal particles from experiment and model at reactant concentration of 0.05 M (a); 0.1 M (b); 0.15 M (c).

4. CONCLUSIONS

A pure superparamagnetic magnetite nanoparticle has been successfully synthesized via the hydrothermal method at 210°C. The crystal diameter was about 9.4–30 nm and particle diameter was lower than 200 nm. From the overall characterization, it was concluded that the time and the concentration of reactants (FeCl_3) affected the growth of magnetite crystals. An increase in reaction time increased the diameter of the crystal and crystallinity. The diameter particle rose with the time due to occurrence of agglomeration. Judging from the trend, magnetite crystal growth in this study followed the Oriented Attachment model, where the lowest concentration of reactant gave the smallest percentage error of 9.6% while the highest concentration contributed to the highest error of 29%. From this study it was suggested: to produce controllable properties of magnetite nanoparticles for drug delivery purpose, low concentrations (0.05 M FeCl_3) was highly recommended.

AUTHOR INFORMATION

Corresponding Author

*Email: fadliunri@yahoo.com

ORCID

Amun Amri : 0000-0001-8896-6405

ACKNOWLEDGEMENTS

Financial support for this study was provided by the Ministry of Research, Technology and Higher Education of Republic of Indonesia (Kemendiknas).

REFERENCES

- [1] Pillai, V.J., I. Jose, and H. Ramachandran. *Early detection of breast cancer using ER specific novel NIR fluorescent dye conjugate: a phantom study using FD-f-DOT system.* in *Optical Tomography and Spectroscopy of Tissue XIII*. 2019. International Society for Optics and Photonics.
- [2] Arruebo, M., et al., *Magnetic nanoparticles for drug delivery.* Nano today, 2007. **2**(3): p. 22-32.
- [3] Mohapatra, M. and S. Anand, *Synthesis and applications of nano-structured iron oxides/hydroxides—a review.* International Journal of Engineering, Science and Technology, 2010. **2**(8).
- [4] Bae, Y.H. and K. Park, *Targeted drug delivery to tumors: myths, reality and possibility.* Journal of controlled release, 2011. **153**(3): p. 198.
- [5] Yu, M., et al., *Dextran and polymer polyethylene glycol (PEG) coating reduce both 5 and 30 nm iron oxide nanoparticle cytotoxicity in 2D and 3D cell culture.* International journal of molecular sciences, 2012. **13** (5): p. 5554-5570.
- [6] Hwang, N.-M., J.-S. Jung, and D.-K. Lee, *Thermodynamics and kinetics in the synthesis of monodisperse nanoparticles.* 2012: InTech Rijeka, Croatia.
- [7] Utami, S., et al. *Crystal-growth kinetics of magnetite (Fe_3O_4) nanoparticles with Ostwald Ripening Model approach.* in *IOP Conference Series: Materials Science and Engineering*. 2018. IOP Publishing.
- [8] Zhang, J., F. Huang, and Z. Lin, *Progress of nanocrystalline growth kinetics based on oriented attachment.* Nanoscale, 2010. **2**(1): p. 18-34.
- [9] Zhang, H. and J.F. Banfield, *Interatomic Coulombic interactions as the driving force for oriented attachment.* CrystEngComm, 2014. **16**(8): p. 1568-1578.
- [10] Łuszczuk, K., J. Kaleta, and R. Mech, *Magnetic core-shell structures as potential carriers in drug delivery system.* J Eng Sci, 2014. **2**(1): p. 1-4.
- [11] Markhulia, J., et al., *Some physical parameters of PEG-modified magnetite nanofluids.* J. Pharm. Appl. Chem, 2016. **2**: p. 33-37.
- [12] Kolhatkar, A., et al., *Tuning the magnetic properties of nanoparticles.* International journal of molecular sciences, 2013. **14**(8): p. 15977-16009.



This article is licensed under a Creative Commons Attribution 4.0 International License.